30 Mar 2001, 10:30 am - 12:30 pm

The Modelling of Free Field Traffic Induced Vibrations by Means of a Dynamic Soil-Structure Interaction Approach

G. Lombaert
University of Leuven - KU Leuven, Belgium

G. Degrande
University of Leuven - KU Leuven, Belgium

THE MODELLING OF FREE FIELD TRAFFIC INDUCED VIBRATIONS BY MEANS OF A DYNAMIC SOIL-STRUCTURE INTERACTION APPROACH

G. Lombaert & G. Degrande
K.U.Leuven, Department of Civil Engineering, Heverlee, Belgium

ABSTRACT

This paper deals with the numerical modelling of free field traffic induced vibrations during the passage of a vehicle on an uneven road. The road unevenness subjects the vehicle to vertical oscillations that cause dynamic axle loads. A simple 2D vehicle model is used for the calculation of the axle loads from the longitudinal road profile. The free field soil response is calculated with the dynamic Betti-Rayleigh reciprocity theorem, using a transfer function between the road and the receiver that accounts for dynamic road-soil interaction. The calculation of the transfer function is based on a dynamic substructure method with a boundary element method for the soil and an analytical beam model for the road. The methodology is finally illustrated by a numerical example where the free field vibrations generated by the passage of a vehicle on a traffic plateau are calculated.

INTRODUCTION

Traffic induced vibrations are a common source of environmental nuisance as they may cause malfunctioning of sensitive equipment, discomfort to people and damage to buildings. They are mainly due to heavy lorries that pass at relatively high speed on a road with an uneven surface. Interaction between the wheels and the road surface causes a dynamic excitation which generates waves that propagate in the soil and impinge on the foundations of nearby structures.

The objective of this paper is to present a numerical model for the calculation of free field traffic induced vibrations (Lombaert et al. 1999, Lombaert et al. 2000). First, it is shown how the dynamic axle loads are computed using simple 2D vehicle models. Second, the transfer functions that describe the dynamic interaction between the road and the soil are derived. Third, these ingredients are used in the dynamic reciprocity theorem to compute the free field response due to a vehicle moving on a road, which uneveness is described in a deterministic way.

THE NUMERICAL MODEL

The modelling of free field traffic induced vibrations is a 3D, dynamic road-soil interaction problem. First, the dynamic axle loads are computed using simple 2D vehicle models. Next, the source-receiver transfer functions between the road and the soil are derived. Finally, these ingredients are used in the dynamic reciprocity theorem to compute the free field response due to a vehicle moving on a road.

The dynamic axle loads

Vehicle models consisting of discrete masses, springs and dampers have often been used and proven good performance (Cebon 1993). As the contribution of vehicle rolling to the dynamic axle loads is expected to be small, a 2D model is sufficient (Cebon 1993). The vehicle body and the wheel axles are generally assumed to be rigid inertial elements, while the primary suspension system and the tires are represented by a spring-dashpot system. The distribution of n axle loads can be written as the summation of the product of Dirac functions that determine the position of the force and a time-dependent function $g_k(t)$:

$$F(x,y,z,t) = \sum_{k=1}^{n} \delta(x)\delta(y - y_k - vt)\delta(z)g_k(t) \quad (1)$$

y_k is the initial position of the k-th axle that moves with the vehicle speed v along the y-axis. As the influence of the road displacements on the dynamic axle loads can be neglected (Cebon 1993), the frequency content $\hat{g}_k(\omega)$ of a single axle load can be calculated as follows from the contribution of n vehicle axles and the road surface profile:

$$\hat{g}_k(\omega) = \sum_{l=1}^{n} \hat{h}_{f_k u_l}(\omega)\hat{u}^l_{w/r}(\omega) \quad (2)$$

$\hat{h}_{f_k u_l}(\omega)$ is the frequency response function (FRF) and represents the frequency content of the axle load at axle k, when a unit impulse excitation is applied to axle l (Cebon 1993, Hunt 1991). $\hat{u}^l_{w/r}(\omega)$ represents the frequency content of the road unevenness applied at axle l, which is calculated from the wavenumber domain representation $\tilde{u}_{w/r}(k_y)$ of the longitudinal road profile $u_{w/r}(y)$:

$$\hat{u}^l_{w/r}(\omega) = \frac{1}{v}\tilde{u}_{w/r}(-\frac{\omega}{v}) \exp(i\omega\frac{y_l}{v}) \quad (3)$$

The range of road unevenness which is important for vehicle dynamics is characterized by wavelengths $\lambda_y = 2\pi/k_y$ between 0.5 m and 50 m. Using equations (2) and (3), the contribution of all axles to a single axle load can be represented by a single FRF $\hat{h}_{f_k u}(\omega)$:

$$\begin{aligned}\hat{g}_k(\omega) &= \frac{1}{v}\tilde{u}_{w/r}(-\frac{\omega}{v})\sum_{l=1}^{n}\hat{h}_{f_k u_l}(\omega)\exp(i\omega\frac{y_l}{v}) \\ &= \frac{1}{v}\tilde{u}_{w/r}(-\frac{\omega}{v})\hat{h}_{f_k u}(\omega) \quad (4)\end{aligned}$$

This equation shows that, for increasing vehicle speed, the quasi-static value of the road profile experienced by the vehicle axles decreases, while the frequency content shifts to higher frequencies.

The road-soil transfer function

The road-soil transfer function $\mathbf{h}_z(x,y,z,t)$ represents the road or soil displacements due to a vertical impulse load on the road. The solution of two subprobems is needed for its calculation. First, the tractions at the road-soil interface are calculated, based on a dynamic substructuring method in the frequency-wavenumber domain. This procedure has been proposed by Clouteau et al. (Clouteau et al. 1994) and is briefly recapitulated here. Next, the displacements at an arbitrary location (x,y,z) at time t are calculated from these soil tractions, resulting in the transfer function $\mathbf{h}_z(x,y,z,t)$.

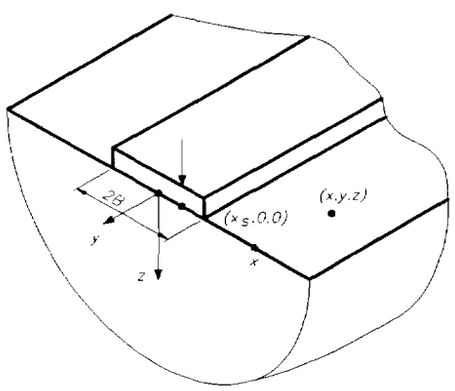

Figure 1: The road-soil interaction problem.

The road is assumed to have a rigid cross section and to be invariant with respect to the longitudinal direction y (figure 1). The road is supported by the soil along the interface Σ_{rs}. From the first assumption it follows that the vertical road displacements $u_{rz}(x,y,t)$ can be written in function of the vertical translation $u_{cz}(y,t)$ of the cross section's centre of gravity and the rotation $\beta_{cy}(y,t)$ about this centre:

$$\begin{aligned} u_{rz}(x,y,t) &= u_{cz}(y,t) + x\beta_{cy}(y,t) \\ &= \boldsymbol{\phi}_r(x)\boldsymbol{\alpha}(y,t) \end{aligned} \tag{5}$$

The displacement modes of the rigid cross section are collected in a vector $\boldsymbol{\phi}_r = \{1,\ x\}^T$, while the vector $\boldsymbol{\alpha}$ collects the displacement u_{cz} and the rotation β_{cy}. The latter can be interpreted as unknown participation factors. The foregoing kinematical assumptions immediately result in the following equilibrium equations for the road, which govern the longitudinal bending and torsional deformations respectively:

$$+EI_x\frac{\partial^4 u_{cz}}{\partial y^4} + \rho A\frac{\partial^2 u_{cz}}{\partial t^2} = f^s_{cz} + f^\delta_{cz} \tag{6}$$

$$-GC\frac{\partial^2 \beta_{cy}}{\partial y^2} + \rho I_p\frac{\partial^2 \beta_{cy}}{\partial t^2} = m^s_{cy} + m^\delta_{cy} \tag{7}$$

In these equations, A is the road's cross section, I_x the moment of inertia with respect to x, C the torsional moment of inertia and I_p the polar moment of inertia; E is the Young's modulus, G the shear modulus and ρ the density of the road. The vertical force per unit length f^s_{cz} and the torsional moment per unit length m^s_{cy} in the right hand side of equations (6) and (7) are the forces exerted by the soil on the road along the interface Σ_{rs}, while f^δ_{cz} and m^δ_{cy} represent a Dirac load applied in a point $(x_S,0,0)$ at time $t=0$.

A double forward Fourier transformation is performed to transform the time t to the circular frequency ω and the longitudinal coordinate y to the horizontal wavenumber k_y. The latter is allowed as the road and the soil are invariant in the y-direction. The displacement decomposition (5) for the vertical road displacements becomes:

$$\begin{aligned} \tilde{u}_{rz}(x,k_y,\omega) &= \tilde{u}_{cz}(k_y,\omega) + x\tilde{\beta}_{cy}(k_y,\omega) \\ &= \boldsymbol{\phi}_r(x)\tilde{\boldsymbol{\alpha}}(k_y,\omega) \end{aligned} \tag{8}$$

In the following, it is understood that a tilde above a variable denotes its representation in the frequency-wavenumber domain so that the arguments k_y and ω can be omitted. The equilibrium equations (6) and (7) become in matrix-vector notation:

$$\left(\tilde{\mathbf{K}}_r - \omega^2\tilde{\mathbf{M}}_r\right)\tilde{\boldsymbol{\alpha}} = \tilde{\mathbf{f}}^s_c + \tilde{\mathbf{f}}^\delta_c \tag{9}$$

with $\tilde{\mathbf{K}}_r$ the stiffness matrix and $\tilde{\mathbf{M}}_r$ the mass matrix of the road and $\tilde{\mathbf{f}}^\delta_c$ the force vector related to the Dirac load. The vector $\tilde{\mathbf{f}}^s_c$ follows from the equilibrium at the road-soil interface Σ_{rs}:

$$\tilde{\mathbf{f}}^s_c = -\int_{\Sigma_{rs}} \boldsymbol{\phi}_r\tilde{t}_{sz}(\tilde{\mathbf{u}}_s)\,d\Gamma \tag{10}$$

$\tilde{t}_{sz}(\tilde{\mathbf{u}}_s)$ is the frequency-wavenumber representation of $t_{sz}(\mathbf{u}_s)$, the vertical component of the soil tractions $\mathbf{t}_s = \sigma_s\mathbf{n}$ on a boundary with a unit outward normal $\mathbf{n}$ for a displacement field $\mathbf{u}_s$.

The continuity of displacements at the road-soil interface results in a decomposition of the soil displacements on the basis of the scattered elastodynamic wave fields $\tilde{\boldsymbol{\phi}}_s$, radiated by the bending and torsional modes of the road:

$$\tilde{\mathbf{u}}_s(x,z) = \tilde{\boldsymbol{\phi}}_s(x,z)\tilde{\boldsymbol{\alpha}} \tag{11}$$

The equilibrium equation (9) can be further elaborated as follows:

$$\left[\tilde{\mathbf{K}}_r - \omega^2\tilde{\mathbf{M}}_r + \int_{\Sigma_{rs}} \boldsymbol{\phi}_r\tilde{t}_{sz}(\tilde{\boldsymbol{\phi}}_s)\,d\Gamma\right]\tilde{\boldsymbol{\alpha}} = \tilde{\mathbf{f}}^\delta_c \tag{12}$$

The solution of this system of equations gives the complex participation factors $\tilde{\boldsymbol{\alpha}}$. The term $\tilde{\mathbf{K}}_r - \mathbf{M}_r$ represents the road impedance, which becomes singular for free bending waves with wave velocity $C_b = \sqrt[4]{EI_x\omega^2/\rho A}$ and free torsional waves with phase velocity $C_t = \sqrt{GC/\rho I_p}$. The integral denotes the soil impedance $\tilde{\mathbf{K}}_s$ and is proportional to the width $2B$ of the road.

A boundary element method is used to calculate the transformed soil tractions $\tilde{\mathbf{t}}_s(\tilde{\boldsymbol{\phi}}_s)$ at the soil-road interface for the scattered wave fields $\tilde{\boldsymbol{\phi}}_s$. The boundary element formulation is based on the formulation of the Betti-Rayleigh reciprocity theorem in the frequency-wavenumber domain, using the Green's functions of a horizontally layered soil (de Barros & Luco 1992, Luco & Apsel 1983). The soil tractions $\tilde{\mathbf{t}}_s(\tilde{\mathbf{u}}_s)$ at the road-soil interface are calculated from the participation factors as $\tilde{\mathbf{t}}_s(\tilde{\boldsymbol{\phi}}_s)\tilde{\boldsymbol{\alpha}}$.

The reciprocity theorem is used for the calculation of the road-soil transfer function $\tilde{\mathbf{h}}_z(\xi_1, k_y, \xi_3, \omega)$ from these soil tractions:

$$\tilde{\mathbf{h}}_z(\xi_1, k_y, \xi_3, \omega) = \int_{\Sigma_{rs}} \tilde{\mathbf{u}}^G(\xi_1 - x, k_y, \xi_3, \omega)\tilde{\mathbf{t}}_s(x, k_y, z = 0, \omega)\, d\Gamma \quad (13)$$

where $\tilde{\mathbf{t}}_s(x, k_y, z = 0, \omega)$ are the soil tractions at the interface z=0 and $\tilde{\mathbf{u}}^G(x, k_y, z, \omega)$ represents the double forward Fourier transformed Green's tensor of a layered half-space. In the load case considered, only the vertical tractions $\tilde{t}_{sz}(x, k_y, z = 0, \omega)$ have a non zero resultant. When the loaded area is small compared to the wavelength in the soil, it can be assumed that the horizontal tractions have a small influence on the free field displacements, so that:

$$\tilde{\mathbf{h}}_z(\xi_1, k_y, \xi_3, \omega) = \int_{\Sigma_{rs}} \tilde{\mathbf{u}}_z^G(\xi_1 - x, k_y, \xi_3, \omega)\tilde{t}_{sz}(x, k_y, z = 0, \omega)\, d\Gamma \quad (14)$$

The response to the moving dynamic axle loads

The dynamic Betti-Rayleigh reciprocal theorem is used to calculate the road or soil response. When the problem geometry is invariant with respect to y, the displacements are calculated as the following convolution integral of the vertical axle loads $g_k(t)$ and the transfer function $\mathbf{h}_z(x, y, z, t)$ between the source and the receiver:

$$\mathbf{u}(x, y, z, t) = \sum_{k=1}^{n} \int_{-\infty}^{t} \mathbf{h}_z(x, y - y_k - v\tau, z, t - \tau) g_k(\tau)\, d\tau \quad (15)$$

The representation of this solution in the frequency-wavenumber domain is equal to:

$$\tilde{\mathbf{u}}(x, k_y, z, \omega) = \tilde{\mathbf{h}}_z(x, k_y, z, \omega) \sum_{k=1}^{n} \hat{g}_k(\omega - k_y v)\exp(ik_y y_k) \quad (16)$$

Note that a frequency shift $k_y v$ is applied to the argument of the interaction force $\hat{g}_k(\omega - k_y v)$, where ω is the frequency at the receiver, while $\omega - k_y v$ corresponds to the frequency emitted at the source. The solution in the space-time domain is found from an inverse transformation of the wavenumber k_y to y and the circular frequency ω to t.

NUMERICAL EXAMPLE

In this example, the vertical free field vibrations, generated by the passage of a truck on a traffic plateau are calculated. First, the dynamic axle loads are calculated from the longitudinal road profile and the vehicle FRF. Next, the dynamic road-soil interaction problem is solved and the receiver transfer functions are calculated. Finally, the vertical free field velocities are discussed.

Figure 2a shows the profile $u_{w/r}(y)$ of the traffic plateau with a height H of 0.12 m, a length L of 10 m and sinusoidal slopes with a length l of 1.20 m. Figure 2b shows the

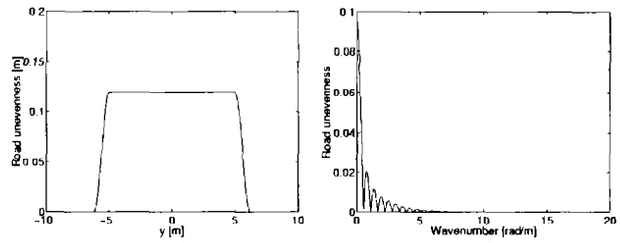

a. $u_{w/r}(y)$. b. $\tilde{u}_{w/r}(k_y)$.

Figure 2: The longitudinal road profile of a traffic plateau with sinusoidal slopes (a) as a function of the coordinate y along the road and (b) in the wavenumber domain.

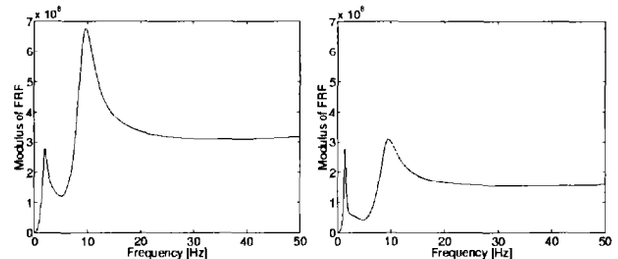

a. $\hat{h}_{f_1 u}(\omega)$. b. $\hat{h}_{f_2 u}(\omega)$.

Figure 3: The vehicle FRF's (a) $\hat{h}_{f_1 u}$ for the rear axle load and (b) $\hat{h}_{f_2 u}$ for the front axle load.

representation of the road profile in the wavenumber domain. The separation between the small lobes in the wavenumber domain is inversely proportional to the mean length $l + L$ of the plateau.

Figure 3 shows the FRF of the dynamic axle loads of a 2D 4DOF vehicle model for a two-axle Volvo FE7 truck (N.N. 1999) with a wheel base of 4 m. The FRF are dominated by the pitch and bounce modes (1.6 Hz and 1.9 Hz) and the axle hop modes (9.1 Hz at the front axle and 9.5 Hz at the rear axle) of the vehicle. These FRF are used to calculate the dynamic axle loads during the passage of the two-axle truck on the traffic plateau at a speed v equal to 14 m/s. Figure 4 shows the time history and the frequency content of both the rear and the front axle load. As the vehicle speed couples the frequency content $\hat{u}^l_{w/r}(\omega)$ to the wavenumber domain representation $\tilde{u}_{w/r}(k_y)$ of the road profile, the spectrum of the axle loads also shows a lobed behaviour.

As the case is considered where the load is applied at the centre of the road ($x_S = 0$), $\beta_{cy} = 0$ since the torsional and bending modes are uncoupled and the following discussion is restricted to the bending deformation of the road.

Road profile				
layer	d	E	ν	ρ
	[m]	[$\times 10^6$ N/m^2]	[-]	[kg/m^3]
asphalt	0.08	25000	0.3	2100
granular	0.17	500	0.5	2000
foundation	0.17	200	0.5	1800

Table 1: Road profile.

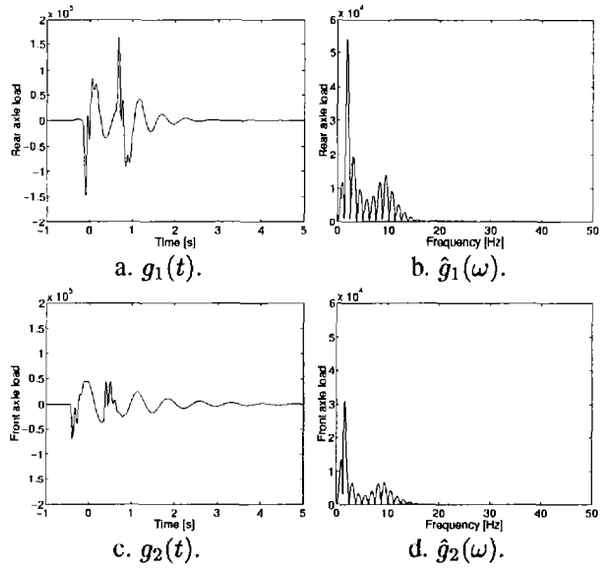

a. $g_1(t)$. b. $\hat{g}_1(\omega)$.

c. $g_2(t)$. d. $\hat{g}_2(\omega)$.

Figure 4: (a) Time history $g_1(t)$ and (b) frequency content $\hat{g}_1(\omega)$ of the rear axle load and (c) time history $g_2(t)$ and (d) frequency content $\hat{g}_2(\omega)$ of the front axle load.

The road has a width $2B = 3\,\mathrm{m}$; it is composed of a bituminous top layer, a granular subbase and a foundation (table 1). The three layer system can be replaced by a single equivalent bituminous layer with a thickness $h = 0.14\,\mathrm{m}$ and a density $\rho = 5910\,\mathrm{kg/m^3}$, which has the same bending stiffness EI and weight ρA as the three layer system.

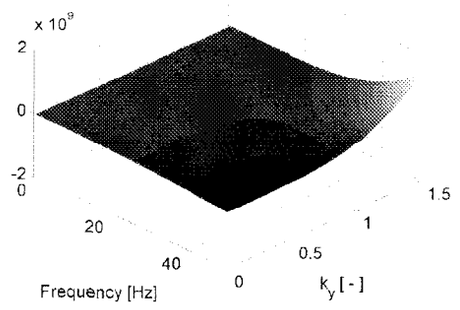

Figure 5: The road impedance for the bending modes.

Figure 5 shows the bending term $\tilde{k}_{r11} - \omega^2 m_{r11}$ of the road impedance as a function of the frequency $f = \omega/2\pi$ and the dimensionless wavenumber $\overline{k}_y = k_y C_S/\omega$ with C_S the shear wave velocity of the supporting soil. At low frequencies and low $\overline{k}_y$, the road mass dominates the road impedance, which is therefore negative; at high frequencies and high $\overline{k}_y$, the bending stiffness term dominates. For dimensionless wavenumbers $\overline{k}_y = C_S \sqrt[4]{\rho A/EI_x\omega^2}$, the road impedance $\tilde{k}_{r11} - \omega^2 m_{r11}$ equals zero.

The soil is represented by a homogeneous halfspace with a density $\rho = 1800\,\mathrm{kg/m^3}$, a shear wave velocity $C_S = 150\,\mathrm{m/s}$, a dilatational wave velocity $C_P = 300\,\mathrm{m/s}$ and a hysteretic material damping ratio $\beta = 0.025$ in shear and volumetric deformation. s represents the ratio of the body wave velocities.

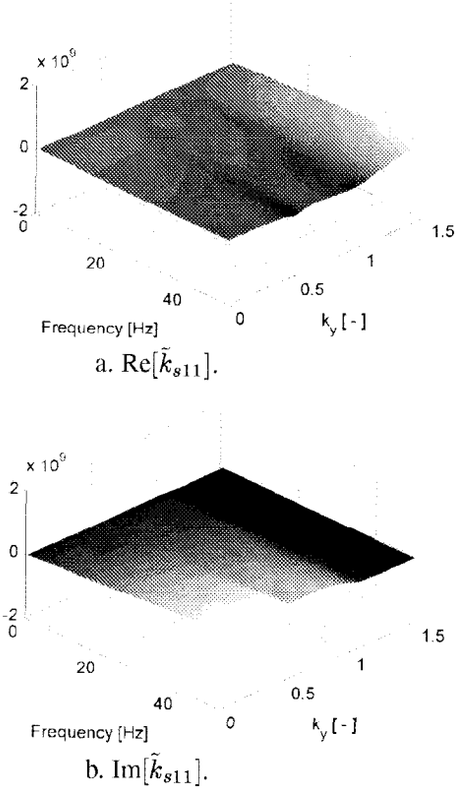

a. $\mathrm{Re}[\tilde{k}_{s11}]$.

b. $\mathrm{Im}[\tilde{k}_{s11}]$.

Figure 6: (a) Real and (b) imaginary part of the soil impedance for the bending modes.

32 boundary elements of equal length $l_e = 0.094\ m$ have been used for the discretization of the road-soil interface. The size of the boundary elements is small compared to the Rayleigh wavelength, but is required for an accurate representation of the peaks of the soil tractions at the edges of the road at $x = \pm B$. Figures 6a and 6b show the real and the imaginary part of the soil impedance $\tilde{k}_{s11}$ of the homogeneous halfspace for the bending modes as a function of the frequency f and the dimensionless wavenumber $\overline{k}_y$. The imaginary part represents the energy dissipation due to radiation and material damping in the soil. The following observations can be made: (1) $0 \leq \overline{k}_y \leq s$: longitudinal, shear and Rayleigh wave propagation takes place. For $\overline{k}_y$ tending to s, the real part of the equivalent stiffness decreases; (2) $s \leq \overline{k}_y \leq 1$: the imaginary part of the stiffness drops as longitudinal waves are inhomogeneous; (3) $1 \leq \overline{k}_y \leq \overline{k}_R$: shear and longitudinal waves are inhomogeneous. At $\overline{k}_y$ close to the Rayleigh wavenumber $\overline{k}_R$, the real part is small; (4) $\overline{k}_R \leq \overline{k}_y$: the real part increases for larger $\overline{k}_y$, while the imaginary part drops to a relatively low value, as energy dissipation takes place through hysteretic material damping only.

The real part of the total impedance is shown in figure 7. Comparison with figures 5 and 6 indicates that the soil impedance dominates the total impedance at low frequencies and wavenumbers. At high frequencies and low

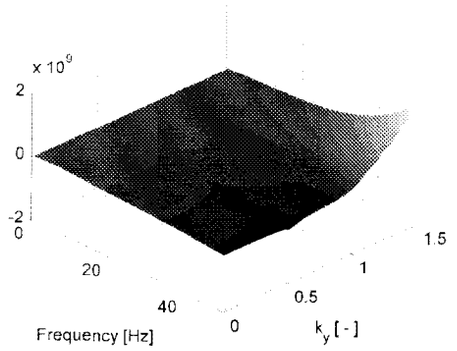

Figure 7: Real part of the total impedance for the bending modes.

wavenumbers, the road mass is important, while at high frequencies and wavenumbers, the bending stiffness of the road has a considerable influence. As both $\tilde{m}_{r11}$ and $\tilde{k}_{r11}$ are real, the imaginary part of the total impedance equals the imaginary part of the soil impedance and energy dissipation only takes place through wave propagation and material damping in the soil.

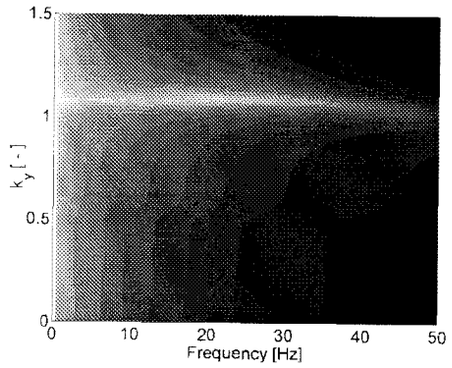

Figure 8: Modulus of $\tilde{u}_{cz}(k_y, \omega)$.

Figure 8 shows a contour plot of the modulus of the displacement $\tilde{u}_{cz}(k_y, \omega)$ at the cross section's centre of gravity and indicates that a coupled road-soil wave propagates at a phase velocity C_{rs} close to the Rayleigh wave velocity C_R in the soil. At low frequencies, C_{rs} is slightly lower than C_R due to the influence of the road mass and no waves are radiated. At $f = C_R^2\sqrt{12\rho/E}/2\pi h = 40.1$ Hz, $C_{rs} = C_b = C_R$. At higher frequencies, the bending stiffness term dominates the road impedance and C_{rs} is larger than C_R, while dissipation takes place through material damping and wave propagation in the soil.

The transfer function between the source and the receiver is calculated from the soil tractions for receivers located at distances of 8 m to 64 m, with steps of 8 m. Figure 9 shows the modulus of the transfer function $\tilde{h}_{zz}(x = 24, \overline{k}_y, z = 0, \omega)$, which decreases for increasing frequencies.

The free field velocities are calculated from the dynamic axle loads and the transfer functions between the road and the soil. Figure 10 shows the time history of the vertical free field velocity as a function of the distance to

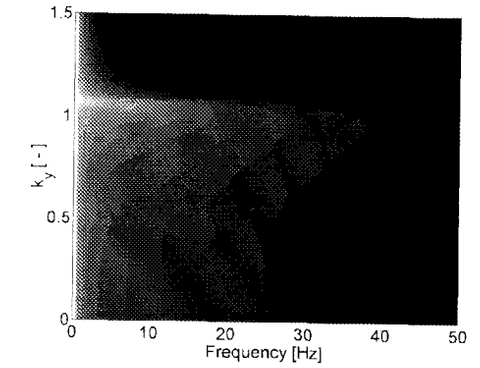

Figure 9: Modulus of $\tilde{h}_{zz}(x = 24, \overline{k}_y, z = 0, \omega)$.

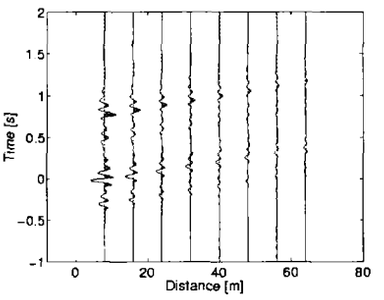

Figure 10: Time history of the vertical free field vertical velocity as a function of the distance to the centre of the road.

the road centre. At $t = 0$, the front axle of the vehicle is situated at the middle of the plateau. It can be observed that wave propagation in the soil delays and attenuates the time signals for increasing distance to the source.

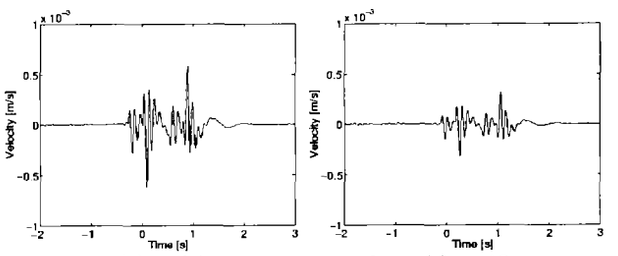

a. $v_z(t)$ at 24 m. b. $v_z(t)$ at 48 m.

Figure 11: Time history of the free field velocity (a) at 24 m and (b) at 48 m of the centre of the road.

Figure 11 shows the time history of the vertical free field velocity at 24 m and at 48 m from the centre of the road. The duration of the transient signal is approximately proportional to the sum of the wheel base and the plateau length and is inversely proportional to the vehicle speed.

Figure 12 shows the frequency content of the vertical free field velocity at 24 m and at 48 m from the centre of the road. The lobed behaviour originates from the wavenumber domain representation of the profile. The frequency content is mainly situated below 15 Hz. When figure 12a and 12b are compared, it can be observed that the frequency

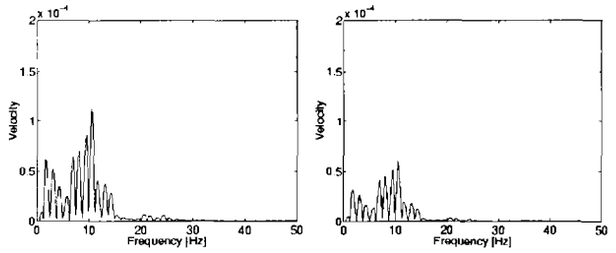

a. $\hat{v}_z(f)$ at 24 m. b. $\hat{v}_z(f)$ at 48 m.

Figure 12: Frequency content of the free field velocity (a) at 24 m and (b) at 48 m of the centre of the road.

content at higher frequencies is stronger attenuated.

CONCLUSION

A numerical model has been presented that enables the calculation of free field traffic induced vibrations. Vehicle transfer functions have been used for the calculation of the dynamic axle loads from the longitudinal road profile and a linear vehicle model. The calculation of the road and soil vibrations is based on an application of the Betti-Rayleigh reciprocity theorem for moving point loads. The transfer function between the road and the receiver in the free field is calculated with a dynamic road-soil interaction model.

ACKNOWLEDGEMENTS

The results presented in this paper have been obtained within the frame of the research project MD/01/040 "The study of determining factors for traffic induced vibrations in buildings". The support of the Prime Minister's Services of the Belgian Federal Office for Scientific, Technical and Cultural Affairs is gratefully acknowledged.

REFERENCES

Cebon, D. (1993), Interaction between heavy vehicles and roads, Technical report, Cambridge University Engineering Department.

Clouteau, D., Aubry, D. & Bonnet, G. (1994), Modeling of wave propagation due to fixed or mobile sources, *in* 'Wave propagation and reduction of vibrations', Bergverlag, Bochum, pp. 109–121.

de Barros, F. & Luco, J. (1992), Moving Green's functions for a layered visco-elastic halfspace, Technical report, Department of Applied Mechanics and Engineering Sciences, University of California, San Diego, La Jolla, California.

Hunt, H. (1991), 'Modelling of road vehicles for calculation of traffic-induced ground vibrations', *Journal of Sound and Vibration* **144**(1), 41–51.

Lombaert, G., Degrande, G. & Clouteau, D. (1999), Deterministic and stochastic modelling of free field traffic induced vibrations, *in* P. Pereira & V. Miranda, eds, 'International Symposium on the Environmental Impact of Road Pavement Unevenness', Porto, Portugal, pp. 163–176.

Lombaert, G., Degrande, G. & Clouteau, D. (2000), 'Deterministic modelling of traffic induced vibrations', *Soil Dynamics and Earthquake Engineering* . Accepted for publication.

Luco, J. & Apsel, R. (1983), 'On the Green's functions for a layered half-space. Part I', *Bulletin of the Seismological Society of America* **4**, 909–929.

N.N. (1999), Vehicle model for a Volvo FE7 truck, Private communication, Volvo.